

The structure of tropical lateritic soils as an impacting factor in the shape of soil-water characteristic curves

Alana Dias de Oliveira^{1#} , Flávia Gonçalves Pissinati Pelaquim¹ ,

Renan Felipe Braga Zanin¹ , Thadeu Rodrigues de Melo² ,

João Tavares Filho² , Avacir Casanova Andrello³ , Raquel Souza Teixeira¹ 

Article

Keywords

Lateritic soils
Filter paper method
Pressure plate method
Soil-water characteristic curve
Porosimetry

Abstract

The presence of unsaturated flow in tropical lateritic soils of unknown hydromechanical behavior may lead to severe geotechnical problems. It is known that soil-water characteristic curves (SWCC) are a valuable tool to define this behavior and facilitate the suction estimation, acting on tests performed with no control of such parameter. This article aimed to determine and model the SWCC for 3 unprecedented tropical soils, in the undisturbed and the compacted conditions, from the Paraná state, located in the south of Brazil. The soils studied are one clay and two sands, all lateritic. The pressure plate and the filter paper methods were used to determine the SWCC. The samples were carved and submitted to the drying paths. Furthermore, Mercury Intrusion Porosimetry (MIP) tests were performed in samples of the studied soils in order to obtain the pore size distribution (PSD), contributing to the bimodal definition of curves and the prediction of SWCC main parameters. Both techniques (pressure plate and filter paper) were combined and the SWCC was adjusted by Gitirana & Fredlund model, which efficiently represents the shape of the traditional curves for tropical soils. Furthermore, the SWCCs were predicted by PSD and obtained satisfactory numerical fits. All SWCC presented air entry values in the macropores that are characteristic of soils as the lateritic, given that its structure was considered a key factor in the shape of the curves.

1. Introduction

Lateritic soils are widely used in civil construction, since they generally present high shear resistance (Sun et al., 2016). However, there are limited research regarding their hydromechanical behavior, soil-water characteristic curves (SWCC) and structure.

The analysis of water retention behavior in the soil is important for various geotechnical engineering applications, being fundamental to comprehend water flow, deformation process and shear resistance in unsaturated soils. The SWCC represents the soil capacity of storing and/or releasing water in the presence of different suctions. The SWCC performs a significant role on estimating hydraulic conductivity, shear parameters and volume variation of unsaturated soils (Vanapalli et al., 1996; Ajdari et al., 2012), becoming, then, an essential component in certain recent constitutive models for unsaturated soils.

According to Fredlund & Rahardjo (1993), the SWCC can be defined as the relation between suction and moisture content or saturation degree. It is usually sigmoid-shaped, though, several authors affirm that the SWCC shape is dependent on few factors, such as the granulometry (Marinho, 2005; Chiu et al., 2012; Carvalho & Gitirana, 2021), the soil structure (Vanapalli et al., 1999; Zhou et al., 2014), the temperature (Chahal, 1965; Romero et al., 2001) and the tension state (Vanapalli et al., 1999; Tavakoli Dastjerdi et al., 2014). According to Gitirana & Fredlund (2004), the pore size distribution might influence the soil-water characteristic curve shape, which may present an “S” shape – unimodal, containing only one dominating pore size – or “Double S” shape – bimodal, containing macro and micropores.

Moreover, the type of soil and structure may directly affect the SWCC shape of undisturbed and compacted soils. This structure can also be represented by the pore

[#]Corresponding author. E-mail address: oliveira.alana@uel.br

¹Universidade Estadual de Londrina, Departamento de Construção Civil, Londrina, PR, Brasil.

²Universidade Estadual de Londrina, Departamento de Agronomia, Londrina, PR, Brasil.

³Universidade Estadual de Londrina, Departamento de Física, Londrina, PR, Brasil.

Submitted on May 6, 2021; Final Acceptance on March 18, 2022; Discussion open until August 31, 2022.

<https://doi.org/10.28927/SR.2022.070521>

 This is an Open Access article distributed under the terms of the Creative Commons Attribution License, which permits unrestricted use, distribution, and reproduction in any medium, provided the original work is properly cited.

size distribution (PSD) obtained through mercury intrusion porosimetry (MIP) (Romero et al., 1999).

Although some researchers report this determination, most of them concern only compacted soil (Vanapalli et al., 1999; Kim & Kim, 2010) or undisturbed soil (Aung et al., 2001; Miguel & Vilar, 2009; Miguel & Bonder, 2012), individually. Therefore, there is a lack of knowledge on gathering both conditions.

This paper aims to verify the influence of soil pore distribution on SWCC of three unprecedented tropical soils from the south of Brazil, determining and modeling it along the drying branch of undisturbed and compacted samples.

2. Materials and methods

2.1 Materials

The lateritic soils used in this study were collected in a range of 2 meters depth from three municipalities of the Paraná state, south region of Brazil: Londrina, Tuneiras do Oeste and Mandaguaçu, as illustrated in Figure 1. The three soils do not have the same geological origin: Londrina's is a residual basalt, Tuneiras do Oeste's is from a geological transition area, between sandstones and basaltic flows, and Mandaguaçu's is a sedimentary soil from a sandstone origin (Gonçalves et al., 2018).

Disturbed and undisturbed samples were collected in the field for laboratory tests, the first being used for compaction according to NBR 7182 (ABNT, 2016), using the Normal Proctor Energy (6 kgf.cm/cm^3). A cylinder 12.7 cm high and 10 cm in diameter was used, where 3 layers of soil of equal masses were sequentially arranged, each one being compacted with 26 blows given by a 2.5 kg and 30 cm high of fall socket. It should be noted that there was scarification of the first and second layers before receiving the next one. The main

characteristics of the soils, as well as the undisturbed and compacted samples used in the tests are presented in Table 1.

2.2 Methods

2.2.1 Mercury intrusion porosimetry (MIP)

Mercury Intrusion Porosimetry (MIP) tests were performed in samples of the studied soils in order to obtain the pore size distribution (PSD), contributing to the bimodal definition of curves and the prediction of SWCC main parameters.

During preparation of soil samples for MIP test, the method of greenhouse drying was used. The greenhouse was chosen because it results in less changes in the intra-aggregate pore shape once the changes of these pores are related to the processes of wetting and drying. Furthermore, due the shorter period of drying, the capacity of the particles to reorganize is limited (Li & Zhang, 2009; Sasanian & Newson, 2013; Otalvaro et al., 2016).

The pore distribution curves were obtained by means of mercury intrusion porosimetry tests (MIP tests) with specimens of about 1 cm of nominal dimensions (ASTM, 2018). The applied mercury pressures ranged from approximately 0.7 to 414000 kPa, with the application of pressure steps until the mercury could no longer be intruded in the soil void volume.

2.2.2 Soil-water characteristic curves (SWCC)

Two different methods were applied to measure the hydromechanical behavior of unsaturated soils for a wide range of suction. For suctions ranging between 10 and 1000 kPa, the pressure plate device was used based on the principle of axis translation, or pressure plate method (PPM). The filter paper method (FPM) was applied to obtain suctions along the entire range of suction values varying between 1 and 10^6 kPa, according to ASTM (2016).

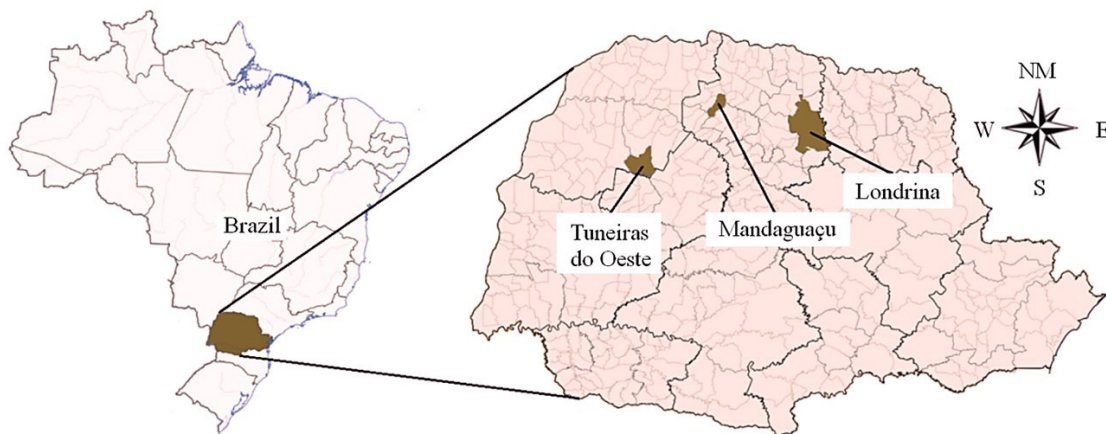


Figure 1. Location of soil collection.

Table 1. Characteristics of three lateritic soils (Cancian et al., 2017; Gonçalves et al., 2017; Gonçalves et al., 2019).

Soil	Londrina	Tunciras do Oeste	Mandaguaçu
Physical indexes			
Specific gravity, G_s	3.03	2.89	2.69
Limit of liquidity (%)	51.0	20.0	31.0
Plasticity index (%)	13.0	7.0	16.0
Particle size distribution with deflocculant – ABNT (1995) and ASTM (2017)			
Sand – $0,06 < f < 2,0$ mm (%)	21.0	74.3	71.0
Silt – $0,002 < \phi < 0,06$ mm (%)	23.5	4.7	15.5
Clay – $\phi < 0,002$ mm (%)	55.5	21.0	13.5
Coefficient of uniformity - C_U	3.3	156,8	148.2
Coefficient of curvature - C_C	0.3	30.2	37.1
Particle size distribution without deflocculant – ABNT (1995) and ASTM (2017)			
Sand – $0,06 < f < 2,0$ mm (%)	20.0	74.3	84.0
Silt – $0,002 < \phi < 0,06$ mm (%)	77.5	23.7	16.0
Clay – $\phi < 0,002$ mm (%)	2.5	2.0	0.0
Coefficient of uniformity- C_U	1.9	50.0	9.5
Coefficient of curvature - C_C	0.3	9.2	2.4
Classifications ⁽¹⁾			
USCS – ASTM (2017)	CM	SC	SM
MCT - Nogami e Villibor (1981)	LG'	LA'	LA'
Mineralogical composition			
Kaolinite (%)	41.9	16.4	13.0
Gibbsite (%)	7.5	-	-
Undisturbed samples characteristics			
Mean molding moisture content (%)	32.0	8.0	3.0
Mean dry density (g/cm^3)	1.14	1.45	1.61
Saturated moisture content (%)	47.0	26.0	19.0
Initial void ratio - e_0	1.7	1.0	0.7
Compacted samples characteristics			
Optimal moisture content (%)	32.4	10.8	14.0
Maximum dry density (g/cm^3)	1.43	1.96	1.86
Saturated moisture content (%)	40.0	17.0	20.0
Initial void ratio - e_0	1.1	0.5	0.4

⁽¹⁾Notes - Classifications: USCS – Unified Soil Classification System; MCT - Miniature, Compacted, Tropical. LG' – Lateritic clay soils; LA' – Lateritic sandy soils.

In PPM and FPM, undisturbed and compacted samples of varied sizes were used, molded with the aid of plastic rings. The size of the specimens for the filter paper method was 21 mm in height and 47 mm in diameter. For the pressure plate method, the specimens were 25 mm in height and 35 mm in diameter.

2.2.2.1 Pressure plate method (PPM)

Part of the pressure plate system is a high air entry (HAE) ceramic plate, covered on one side by a thin neoprene diaphragm, secured to the edges of the plate. The diameter of the ceramic plate was 280 mm and can support up to 15 bars (1500 kPa). This system operates based on the principle of shaft translation, which involves increasing the air pressure (u_a), keeping the water pressure (u_w) (Marinho et al., 2008).

Four specimens of each condition (undisturbed and compacted) from each soil were previously saturated by

capillary action and placed on the HAE plate inside the pressure cell. The tests were carried out increasing the matric suction from 10 to 300 kPa in several steps. When the amount of water in the sample reached equilibrium then the next level of suction could be applied. Equilibrium was considered reached after the constant mass of the specimens, meaning that for that pressure there was no longer a pore size prone to losing water.

2.2.2.2 Filter paper method (FPM)

The principle about FPM is that after balancing, the soil and paper suction are the same. Filter paper is a porous material and as such can retain water like soil (Chandler et al., 1992). Basically, filter paper achieves equilibrium with the soil through vapor (total suction) or liquid flow (matric suction).

For the experimental points of the SWCCs to be representative of the drying branch, it was decided to control

the masses of the specimens over time while drying in the open air, using a 0.0001g precision scale. That is, estimates were made about the weight of the specimens for several different moisture contents. As soon as the weighing indicated the calculated mass, it would be verified that it had reached the desired moisture content.

Ten specimens of each condition (undisturbed and compacted) of each soil were previously saturated and the partial air-drying process began. For the measurement of matric suction, each specimen received two Whatman n° 42 filter papers, one under and one over the specimen. Total suction was not measured in this study. Each filter paper was cut so that when placed in contact with the specimen, its entire surface would remain in contact with it without interference from the plastic ring.

After assembly, the set was wrapped in plastic film and then in aluminum foil. The packaging process was necessary to guarantee the balance of the specimens with the filter paper without external interference (unforeseen loss or gain of moisture). In addition, the specimens were placed in a polystyrene box to keep the temperature controlled for 21 days, based on Marinho (1997).

With the balance of the water potential between the filter paper and the specimen, it was possible to measure their

volumetric moisture contents. The filter paper technique obtains the matric suction indirectly, using for this determination the correlations proposed by Chandler et al. (1992), as shown in Equations 1 and 2.

$$w_{paper} \leq 47\% \rightarrow \Psi_{paper} = 10^{(4,84 - 0,0622 \cdot w_{paper})} \quad (1)$$

$$w_{paper} > 47\% \rightarrow \Psi_{paper} = 10^{(6,05 - 2,48 \cdot \log w_{paper})} \quad (2)$$

Where Ψ_{paper} is the suction of the filter paper in (kPa), and w_{paper} is the volumetric moisture content of the filter paper in (%).

3. Results

3.1 MIP test results and SWCCs in the full suction range

Figure 2 presents the PSD and the cumulative distribution of undisturbed and compacted samples for CM, SC and SM soils. In Figure 2a, all three undisturbed soils exhibit distinct bimodal PSD, given its first peak next to 0.01 μm for CM

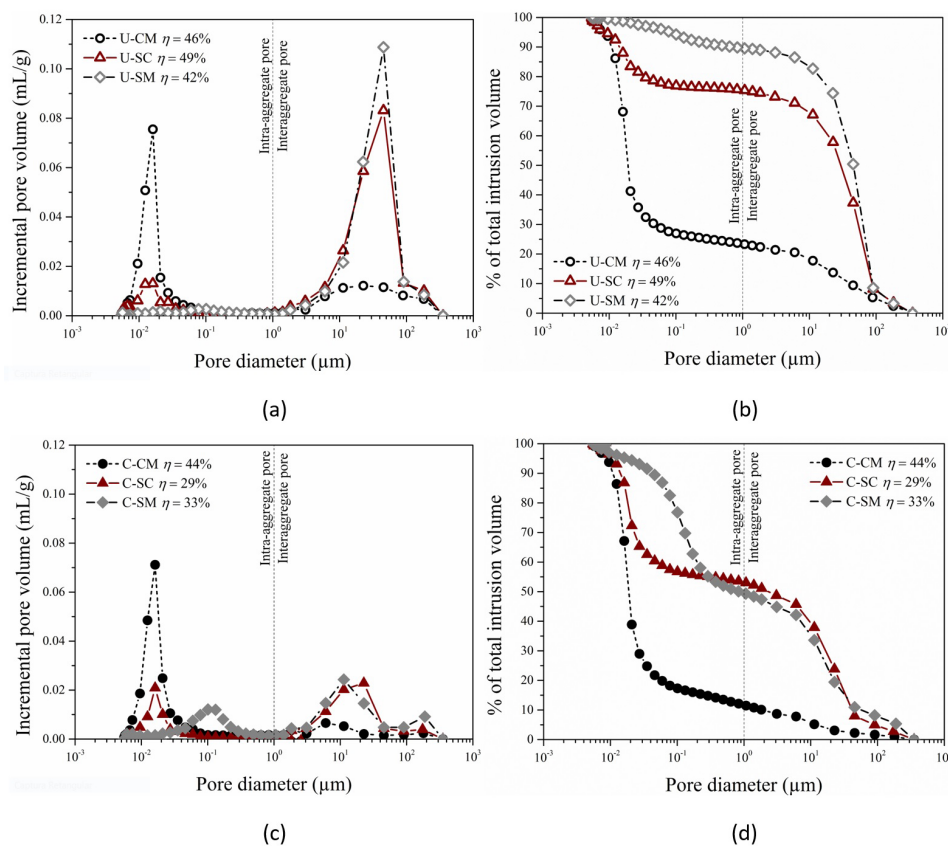


Figure 2. PSD of undisturbed samples (a) incremental pore volume and (b) cumulative % of total intrusion volume; and compacted samples (c) incremental pore volume and (d) % of total intrusion volume.

and SC samples, and near to 0.1 μm for SM sample. The second peak for all samples of soils is located between 10 and 100 μm .

For all three unsaturated compacted soils, illustrated in Figure 2c, it was also verified bimodal PSD with first peak next to 0.01 μm for CM and SC samples, and close to 0.1 μm for SM sample. The second peak is observed for all three soil samples between 1 and 10 μm . It should be noted that the trimodal behavior observed in SM compacted soils is probably due some failure during MIP, as clarified by Sasanian & Newson (2013).

The tendency in the PSD observed in Figure 2 defines the existence of two main pore families: intra-aggregate (diameter until 1 μm) and interaggregate (diameter greater than 1 μm), as cited by Gutierrez et al. (2008) and Li & Zhang (2009). The authors explain that the intra-aggregate pores are formed from the composition of mineral agglomerates and the interaction between them in the clayey matrix of the soil, while the interaggregate pores are characterized by conditioning the structural porosity, that is, they are related to the arrangement of the grains in themselves. The existence of a separation interval between the dominant pores observed, is a particular characteristic of lateritic soils very weathered in Brazil, noted also by Miguel & Bonder (2012) and Otalvaro et al. (2016).

The amount of PSD with a diameter of up to 1 μm , intra-aggregate, was more expressive for the CM soil sample than for the others (SC and SM), which was expected due to the more clayey character and the recognized microaggregation of this soil (Gonçalves et al., 2019).

Comparing the compacted and undisturbed samples, the CM curves showed a similar trend (especially for the intra-aggregate pores), even under different initial void indices (1.7 and 1.1, respectively). The finding that compaction has practical implications only in pores with larger soil diameters had already been reported by several authors (Delage et al., 1995; Simms & Yanful, 2001; Sun et al., 2016; Gao & Sun, 2017). This result implies that the porosity (the relationship between the void volume and the sample volume) of the CM soil remains practically unchanged with the use of compaction. On the other hand, the expressive variation of interaggregate pores for SC and SM is a direct result of the restructuring process, with a consequent decrease in porosity, for the same reason.

It is noteworthy that for CM soil the compaction process increased the discrepancy between intra and interaggregate pores (with the evident maintenance of the first family and reduction only in the second) and for SC and SM soils there is an equivalence between the proportion of the volume of pores, with differences of less than 15% between them. Furthermore, the percentage difference between the intra-aggregate pores, when going from undisturbed to compacted condition, for all three soils (CM, SC and SM) was 13, 25 and 44%, respectively. This allows us to conclude that the transition of pore volume from inter to intra-aggregate due to

compaction is more expressive, as the soil is more granular and/or has a lower clay fraction.

Finally, the total intrusion volume for CM for the undisturbed and compacted conditions is clearly lower than the values for SC and SM, as can be seen in Figure 2b and 2d. According to Nimmo (2005), this occurs because the formation of intra-aggregate pores occurs in the clay soil matrix, which is considerably larger in CM soil than in the others. Thus, a higher intra-aggregate pores amount caused a lower amount of mercury intruded into the CM soil.

From the determination of the pore distribution as bimodal for all three soils studied, both in the undisturbed and compacted condition, it is possible to predict that the variation in the volumetric moisture content and/or the saturation degree with the soil suction will have the existence of transition zones, with intermediate and well-defined levels characterized by low variation in moisture content for a wide range of suction. This shape corresponds to the typical shapes of a bimodal soil, like the shapes obtained by Burger & Shackelford (2001) and Carvalho et al. (2002).

Figure 3 shows the results obtained by the drying process using the PPM and FPM methods for undisturbed and compacted soils. Some of the points resulting from the different methods for the same suction values do not coincide perfectly, however, the discrepancy is low, enabling the assertive inference of the curve. It is noteworthy that the samples tested had similar void ratios (with coefficients of variation lower than 10% for undisturbed soils and 5% for compacted soils). This implies considering that the observed discrepancies are restricted to factors such as intrinsic structural differences and the uncontrollable heterogeneity of the material itself.

It is recognized that the shape of the SWCC depends on both the pore size distribution and the particle size distribution. Gerscovich (2001) indicates that sandy soils tend to show a sudden loss of moisture when suction exceeds AEV_1 , while clayey soils tend to have smoother curves. Thus, considering the percentages of particle size fractions, the behavior mentioned was evidenced for the soils in this study.

Furthermore, the same author emphasizes that, with a less considerable influence, the same behavior can be expected when comparing characteristic curves of uniform soils and well-graded soils, respectively.

For an adequate adjustment to the behavior of soils that present micro and macro structures composed of clay aggregates, typical of tropical and subtropical environments, the bimodal model proposed by Gitirana & Fredlund (2004) is recommended. Its application is shown in Figure 3 together with the sampling points. Table 2 shows the parameters of the model by Gitirana & Fredlund (2004), obtained from these curves. The results suggest good fits of the experimental data to the model of Gitirana & Fredlund (2004) with the presented parameters (coefficients of determination R^2 all above 0.9).

As already mentioned in the presentation of the porosimetry results, soil compaction decreased the amount

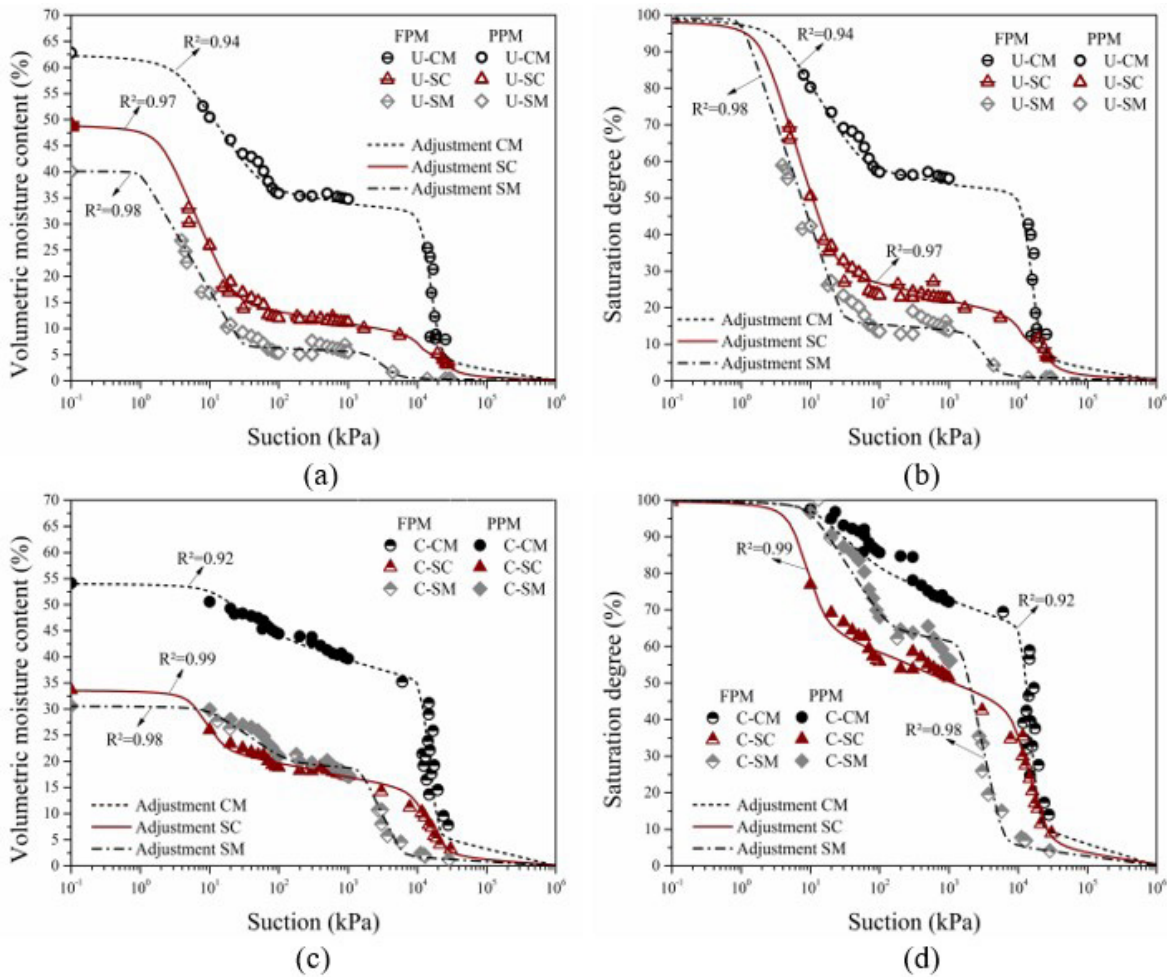


Figure 3. SWCC in the drying branch for a wide suction range: (a) and (c) volumetric moisture content and (b) and (d) saturation degree, respectively.

Table 2. SWCC parameters for three compacted and undisturbed lateritic soils.

Soil sample	1 st Portion				2 nd Portion				a
	θ_{sat} (%)	AEV_1 (kPa)	Ψ_{res1} (kPa)	Sr_{res1} (%)	AEV_2 (kPa)	Sr_{b2} (%)	Ψ_{res2} (kPa)	Sr_{res2} (%)	
U-CM	63	4	45	55	12000	53	20000	5	0.08
U-SC	49	2	21	27	13000	20	22000	0.1	0.09
U-SM	40	1	30	16	2000	14	5000	1	0.02
C-CM	54	12	70	80	11000	66	20000	10	0.04
C-SC	34	6	13	63	10000	45	21000	4	0.10
C-SM	31	10	170	63	1500	62	6000	6	0.04

of interaggregated pores, implying a decrease in the amount of water needed to saturate the soil. Can this be noticed in the θ_{sat} presented in Table 2, where the saturation moisture values for compacted soils are lower than for undisturbed soils, for all soils.

The two AEV found corroborate the ranges of values as a function of particle size presented by Aubertin et al. (1998). It is noteworthy that this statement is true only when particle size analysis is used regardless of the deflocculant.

Undisturbed soils with a higher percentage of fines had typically higher AEV_1 than for those with a lower percentage, in agreement with Vanapalli et al. (1999). For compacted soils, this trend was not evidenced, since for SM soil the AEV_1 obtained was superior to that of SC and practically equal to that of CM.

This C-SM sample's behavior may be related to the intra-aggregate pore size density and, consequently, to the mercury total intrusion volume. After the compaction process,

the pore size density of all soil samples has changed. A higher variation of total intrusion volume is observed for SM (from 10% to 50%) than for SC (from 25% to 45%) and CM (from 75% to 90%). This way, as shown in Figure 2, SM soil assumes a higher quantity of intra-aggregates compared to SC soil. Therefore, for compacted soils the pore size density seems to impact AEV_1 more than the presence of fines.

Regarding AEV_2 , it was noted that they were higher for soils with a higher clay fraction, however, not proportionally for undisturbed soils. When observing the two structures, for each type of soil, a certain similarity is observed, indicating again that the proportion of initial voids does not affect the water-soil characteristic curve at high suction, as discussed in this article (Gao & Sun, 2017). Furthermore, similar AEV_2 values, especially for CM and SC, indicate that there was an influence of the similar mineralogical composition of the studied soils (Gonçalves et al., 2017), since this is the suction range where the adsorption effects occur (Romero et al., 1999).

For undisturbed soils, the trend is evident that the more granular the soil, the lower the values of Sr_{res1} , which is in accordance with the theory of water adsorption by specific surface area of the particles (the larger the effective particle diameter, smaller specific surface area, less possibility of water adsorption). As for the compacted soils, a higher value of Sr_{res1} was also found for the CM soil, as expected, however, the values for the two sandy soils (SC and SM) were coincident. Possibly the explanation for this is correlated to the fact that the pore distribution for these two soils, after the use of compaction, has remained practically the same (percentage difference between the interaggregate pores after compaction equal to 3%).

As explained by Carvalho & Leroueil (2004), regardless of the initial void ratio that a soil sample may have, there is the possibility of presenting a characteristic suction curve that

is unique, removing the interference of this parameter from the assessment. This means that even if two specimens of the same soil initially have different void ratios, the parameter “ $e \times Sr$ ” appears as a constant, unless other factors intervene, such as structural differences (for example, undisturbed and compacted samples), cementation breakage with pore distribution variation or the hysteresis phenomenon itself. To obtain the transformed SWCC, Figure 4 shows the relationships between $e \times pF$ (which is the logarithm of suction in $cm.H_2O$) and the saturation degree (S_r). It is noteworthy that such curves were obtained from those previously defined by Gitirana & Fredlund model (2004), which presented satisfactory adjustments to the experimental data.

Silva et al. (2020) and Carvalho & Gitirana (2021) explain that for deeply weathered soils, the quantity and distribution of pores define the slope of the plateau present in the transformed SWCC ($e \times pF$ versus saturation degree). The smoother this slope, the greater the amount of interaggregate pores. For the studied soils, it is possible to notice that the curves of undisturbed soils presented levels with lower slopes than the curves of compacted soils. This once again confirms the decrease in interaggregated pores because of compaction.

In addition, it is highlighted that the curves presented can be taken as generic for any analyzes that require the estimation of the suction of unsaturated specimens for the studied soils and conditions, even if the samples have a slight variation in the initial void ratio, safeguarding only the possible interferences of the drying and moistening cycles.

3.2 SWCC predicted by PSD

In MIP test, it is assumed the soils contain pores with diameter (d) in the shape of cylindrical flow channels, which are filled with mercury under a determined pressure

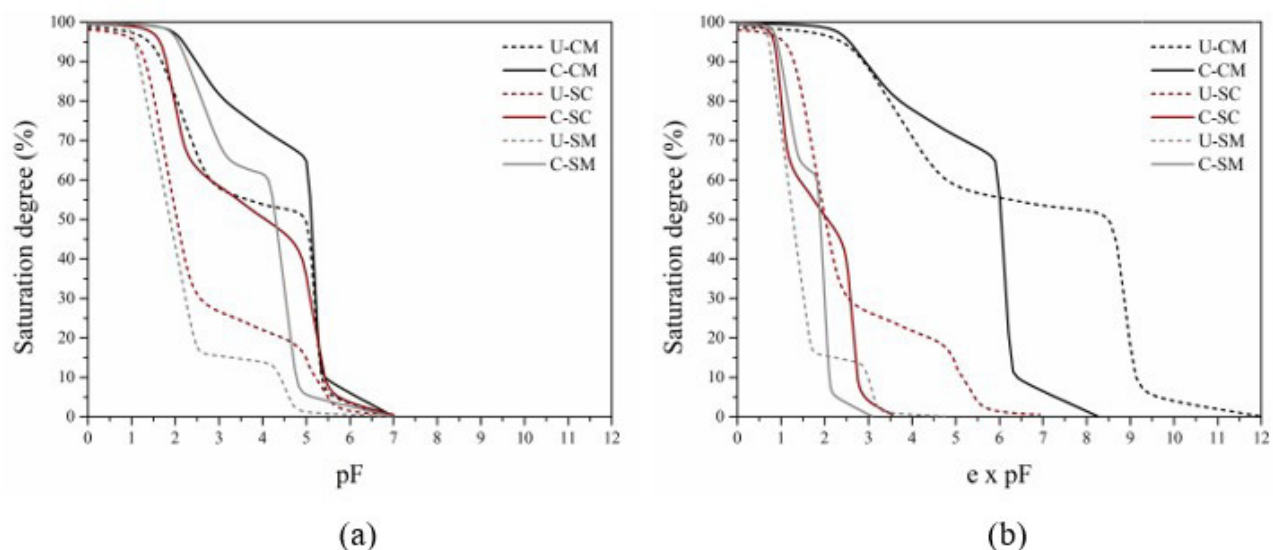


Figure 4. SWCC transformed in the drying arm for a wide range of suction versus saturation degree.

application. The necessary pressure to completely fill the pores with mercury is inversely proportional to the pore size. This relation was firstly pointed by Washburn (1921), and it is shown in Equation 3:

$$P = \frac{4\sigma_{Hg} \cos \alpha_{Hg}}{D} \quad (3)$$

Where D is the pore diameter in (μm), σ_{Hg} is the air/mercury surface tension of 0.484 N/m , α_{Hg} is the contact angle, assumed as 140° (Otalvaro et al., 2016), and P is the pressure in (kPa). As σ_{Hg} and α_{Hg} are constants, the application of a known pressure produces the dimension of corresponding pores.

Some researchers as Delage et al. (1995), Aung et al. (2001), Simms & Yanful (2001), Zhang & Li (2010) and Mascarenha et al. (2010), affirm that the mercury intrusion in a porous medium occurs similarly to the application of pressure in a saturated soil, in other words, like the drying curve of the SWCC. Therefore, according to Otalvaro et al. (2016), the suction may be obtained by replacing the pressure in Equation 4:

$$(u_a - u_w) = \frac{4\sigma_w \cos \alpha_w}{D} \quad (4)$$

Where $(u_a - u_w)$ is the matric suction in (kPa), σ_w is the surface tension of the interface air/water of 0.073 N/m at 20° C , according to Fredlund & Rahardjo (1993), α_w is the contact angle assumed as zero, according to Philip & De Vries (1957). Considering the diameters of the Equations 3 and 4 as similar, the relation $P \approx 5.10 (u_a - u_w)$ is attainable. Thus, it is possible to convert mercury intrusion pressure into matric suction.

With this premise, works such as those by Sun et al. (2016) sought a simplified approach for predicting the soil characteristic curve using only the results of MIP tests. According to the authors, good fits were found for compacted soils by predicting AEV_1 or AEV_2 from the estimated suction for the pore diameter at the region peak of inter or intra-aggregate, respectively. Despite the same authors emphasizing that the predictions for undisturbed soils may be less accurate, especially for those with a high content of

finer, given the possibility of contraction and the appearance of cracks in the specimen during drying, the same technique was applied here, since two of all three soils studied were characterized as sandy.

Table 3 presents the AEV_1 and AEV_2 estimated by the method of Sun et al. (2016). It is observed that the AEV_1 for the soil with higher fines content remained higher than the others, regardless of the condition. However, considering the adjustment shown in Figure 5, all estimated values were higher than those obtained. For the AEV_2 values, a numerical trend was noted like the adjustment of the curve by Gitirana & Fredlund (2004), but in this case with estimated values lower than those obtained. For practical purposes, discrepancies suggest that the simplification, although imprecise, may be acceptable.

Regarding the slope of different parts of the curves, Sun et al. (2016) points out that the peak in the interaggregated pore zone can determine the slope of the first segment of the SWCC, the intra-aggregate pore peak is related to the slope of the third segment, and the flat segment between the two peaks influences the slope of the middle segment in the SWCC.

Thus, according to the authors, a cumulative distribution function (called $F_{(d)}$) represents the volume of pores with diameters greater than d in a gram of dry soil. $F_{(d)}$ can be determined based on the results of MIP tests showed in Figures 2b and 2d and the saturation degree in one gram of dry soil (S_e) is given by Equation 5:

$$S_e = 100 \times \frac{S_r - S_{re}}{100 - S_{re}} \quad (5)$$

Where $S_{re} = 100(e_a - e_e) / e_a$ with e_a being the void ratio before MIP tests, $e_e = \rho_w \cdot F_{(d_{min})} \cdot G_s$ and $F_{(d_{min})}$ is the accumulated volume of mercury for the smallest diameter measured by MIP test, and G_s is the specific gravity. From the parameters obtained (Table 3), the curves predicted by the PSD results of this study are shown in Figure 5.

The coefficients of determination indicate good fits between the data predicted by the PSD and those adjusted by Gitirana & Fredlund (2004) model, both in the undisturbed and compacted conditions. For SC and SM soils, both with a sandier character, the forecast for undisturbed samples was

Table 3. Estimated parameters for prediction of SWCC by PSD - Sun et al. (2016).

Soil sample	AEV_1 (kPa)	AEV_2 (kPa)	G_s	e_a	$F(d_{min})$
U-CM	10	15000	3.08	0.9	0.28
U-SC	5	15000	3.46	1.0	0.29
U-SM	5	2400	2.81	0.7	0.26
C-CM	40	15000	3.14	0.8	0.25
C-SC	10	15000	2.85	0.4	0.14
C-SM	20	2000	2.96	0.5	0.17

Note: Data G_s , e_a and $F(d_{min})$ obtained in MIP tests reports.

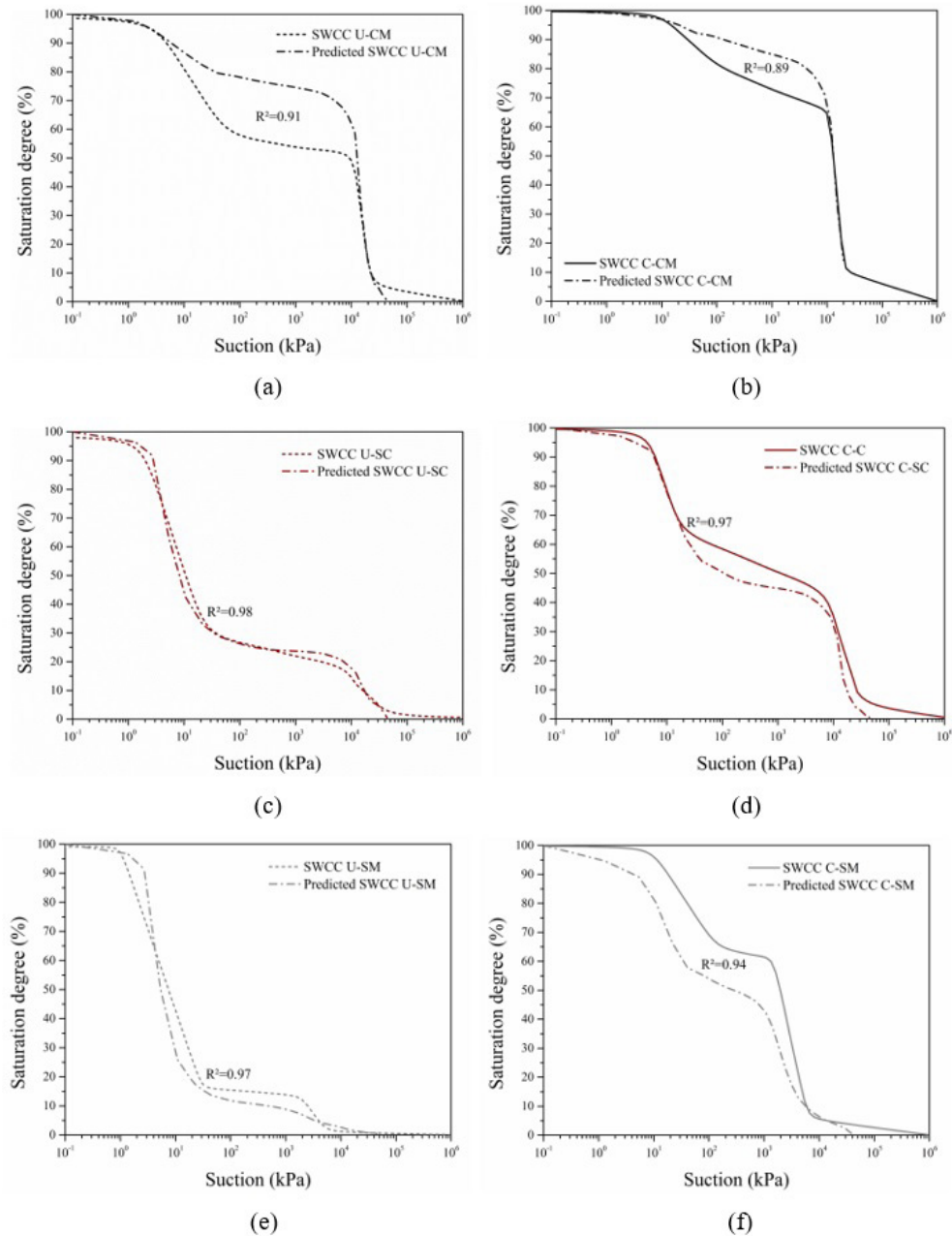


Figure 5. SWCC adjusted and predicted results in drying arm for a wide range of suction *versus* saturation degree.

better than compacted samples, contrary to what was presented by Sun et al. (2016), who described better adjustments for the compacted condition.

On the other hand, the CM soil, despite the satisfactory numerical fit, did not show agreement between the shape of the adjusted and predicted curves for the interaggregated pore region and transition zone. The explanation for this may also be related due to the significant difference between the values of e_0 and e_a that was evidenced. Yan et al. (2021) emphasizes that the SWCC of clayey soils can present inaccuracy when transformed directly from the PSD. This

is because the pore structure changes with suction during the SWCC test, while in the test to obtain the PSD, this characteristic remains constant.

Furthermore, still explaining the prediction behavior for the CM soil, according to Campos et al. (2017), MIP test presents high precision in the quantification of open pores, but does not allow the detection of closed pores, in addition to compressing the material, which may change the actual pore sizes. Therefore, it is reasonable to say that for a soil with a considerable number of fines and micro-aggregation, characteristics of the CM soil (Teixeira et al., 2010;

Gonçalves et al., 2017), the test itself may have influenced the underestimated determination of voids characteristic of intra-aggregates pores, smoothing the curve.

4. Conclusions

There were obtained SWCC for compacted and undisturbed samples of three tropical lateritic soils of the south of Brazil, in addition to MIP tests aiming to study the soil structure. The following conclusions were achieved:

1. The SWCC of compacted and undisturbed samples for CM, SC and SM soils present similar shape to the usual bimodal SWCC (noting the presence of macro and micropores in the soil mass), when using both suction measuring methods. The AEV values of undisturbed samples were reasonably low during the desaturation of macropores, due to the aggregation of fine particles that result in greater pore sizes. The granulometric distribution curves obtained without using deflocculant during the sedimentation phase indicated this microaggregation.
2. The undisturbed samples for all three soil types exhibit distinct bimodal PSD. The compacted samples present similar bimodal PSD for sandy soils, given that clayey soil is different due to its considerable content of fines. The void ratio variation for CM soil, which occurs by the compaction process, alters only the interaggregate pore volume, while the intra-aggregate pore volume remains nearly unaltered.
3. The SWCCs predicted by PSD obtained satisfactory numerical fits when comparing with those adjusted by Gitirana & Fredlund model. The SC and SM soils forecast for undisturbed samples was better than for compacted samples. The CM soil did not show agreement between the shape of the adjusted and predicted curves for the interaggregated pore region and transition zone.

Acknowledgements

The authors thank the Coordination of Improvement of Higher Education Personnel (CAPES) for funding the research.

Declaration of interest

The authors have no conflicts of interest to declare. All co-authors have observed and affirmed the contents of the paper and there is no financial interest to report.

Authors' contributions

Alana Dias de Oliveira: conceptualization, data curation, formal analysis, investigation, writing – original draft. Flávia

Gonçalves Pissinati Pelaquim: investigation, data curation, writing – review & editing. Renan Felipe Braga Zanin: investigation, data curation, writing – review & editing. Thadeu Rodrigues de Melo: resources, supervision. João Tavares Filho: resources, supervision. Avacir Casanova Andreollo: data curation, formal analysis, investigation, resources. Raquel Souza Teixeira: funding acquisition, methodology, resources, supervision, validation, writing – review & editing.

List of symbols

a	Parameter of Gitirana & Fredlund model (2004)
AEV_1	Air entry value of the 1 st portion (kPa)
AEV_2	Air entry value of the 2 nd portion (kPa)
C	Compacted
C_C	Curvature coefficient
C_{NU}	Non-uniformity coefficient
CM	Clayey silt
D	Pores diameter (μm)
e_0	Initial void ratio
e_a	Void ratio before MIP
e_e	Accumulated volume of mercury for the smallest diameter measured by MIP
$F(d)$	Cumulative distribution function
$F(d_{min})$	Accumulated volume of mercury for the smallest diameter measured by MIP
FPM	Filter paper method
G_s	Specific gravity
HAE	High Air Entry
LA'	Lateritic sandy soils
LG'	Lateritic clay soils
MCT	Miniature, Compacted, Tropical.
MIP	Mercury intrusion porosimetry
P	Pressure (kPa)
pF	Logarithm of suction ($\text{cm.H}_2\text{O}$)
PPM	Pressure plate method
PSD	Pore size distribution
R^2	Coefficient of determination (adjustment)
SC	Sandy clay
SM	Sandy silt
S_r	Saturation degree (%)
S_e	Saturation degree in one gram of dry soil (%)
$S_{r,b2}$	Saturation of the beginning of the 2 nd portion (%)
$S_{r,res1}$	Residual saturation of the 1 st portion (%)
$S_{r,res2}$	Residual saturation of the 2 nd portion (%)
SWCC	Soil-water characteristic curve
U	Undisturbed
USCS	Unified Soil Classification System
u_a	Air pressure (kPa)
u_w	Water pressure (kPa)
w_{paper}	Content of water of the filter paper (%)
α_{Hg}	Contact angle of the air/mercury ($^\circ$)
α_w	Contact angle of the air/water ($^\circ$)
θ_{sat}	Saturation volumetric moisture content (%)
ρ_w	Water specific gravity (g/cm^2)

σ_{Hg}	Surface tension of the air/mercury (N/m)
σ_w	Surface tension of the air/water (N/m)
Ψ_{paper}	Suction of the filter paper (kPa)
Ψ_{res1}	Residual suction of the 1 st portion (kPa)
Ψ_{res2}	Residual suction of the 2 nd portion (kPa)

References

- ABNT NBR 6502. (1995). *Rocks and soils - Terminology*. ABNT – Associação Brasileira de Normas Técnicas, Rio de Janeiro, RJ (in Portuguese).
- ABNT NBR 7182. (2016). *Soil - Compaction test*. ABNT – Associação Brasileira de Normas Técnicas, Rio de Janeiro, RJ (in Portuguese).
- Ajdari, M., Habibagahi, G., & Ghahramani, A. (2012). Predicting effective stress parameter of unsaturated soils using neural networks. *Computers and Geotechnics*, 40, 89-96. <http://dx.doi.org/10.1016/j.compgeo.2011.09.004>.
- ASTM D2487-17. (2017). *Standard practice for classification of soils for engineering purposes (unified soil classification system)*. ASTM International, West Conshohocken, PA. <https://doi.org/10.1520/D2487-17>
- ASTM D4404-18. (2018). *Standard Test Method for Determination of Pore Volume and Pore Volume Distribution of Soil and Rock by Mercury Intrusion Porosimetry*. ASTM International, West Conshohocken, PA. <https://doi.org/10.1520/D4404-18>
- ASTM D5298-16. (2016). *Standard test method for measurement of soil potential (suction) using filter paper*. ASTM International, West Conshohocken, PA. <https://doi.org/10.1520/D5298-16>
- Aubertin, M., Ricard, J., & Chapuis, R.P. (1998). A predictive model for the water retention curve: application to tailings from hard-rock mines. *Canadian Geotechnical Journal*, 35(1), 55-69. <http://dx.doi.org/10.1139/t97-080>.
- Aung, K.K., Rahardjo, H., Leong, E.C., & Toll, D.G. (2001). Relationship between porosimetry measurement and soil-water characteristic curve for an unsaturated residual soil. *Geotechnical and Geological Engineering*, 19, 401-416. <http://dx.doi.org/10.1023/A:1013125600962>.
- Burger, C.A., & Shackelford, C.D. (2001). Evaluating dual porosity of pelletized diatomaceous earth using bimodal soil-water characteristic curve functions. *Canadian Geotechnical Journal*, 38(1), 53-66. <http://dx.doi.org/10.1139/t00-084>.
- Campos, J.V., Lavagnini, I.R., Ferreira, J.A., Montrazi, E.T., Bonagamba, T.J., & Pallone, E.M.J.A. (2017). Comparative analysis between different porosimetric tests on macroporous alumina. *Revista Matéria*, 22(1): e11929 (in Portuguese). <https://doi.org/10.1590/S1517-707620170005.0265>
- Cancian M.A., Cancian V.A., Teixeira R.S., Fontenele H.B., & Costa Branco C.J.M. (2017). Influence of moisture content, porosity and time interval until application of the soil-cement mixture on road pavement. *Transportes*, 25(1), 41-50 (in Portuguese). <https://doi.org/10.14295/transportes.v25i1.1126>
- Carvalho J.C., & Gitirana G.F.N. (2021). Unsaturated soils in the context of tropical soils. *Soils and Rocks*, 44(3), e2021068121. <https://doi.org/10.28927/SR.2021.068121>
- Carvalho, J.C., & Leroueil, S. (2004). Transformed soil-water characteristic curve. *Soils and Rocks*, 27(3), 231-242 (in Portuguese).
- Carvalho, J.C., Guimarães, R.C., & Pereira, J.H.F. (2002). Courbes de rétention d'eau d'un profil d'alteration. In J.F.T. Jucá, T.M.P. Campos & F.A.M. Marinho (Eds.), *Proc. 3rd International Conference on Unsaturated Soils* (pp. 289-294), Recife, Brazil. Swets & Zeitlinger (in French).
- Chahal, R.S. (1965). Effect to temperature and trapped air on matric suction. *Soil Science*, 100(4), 262-266.
- Chandler, R.J., Crilly, M.S., & Montgomery-Smith, G. (1992). A low-cost method of assessing clay desiccation for low-rise buildings. *Proceedings of the Institution of Civil Engineers: Civil Engineering*, 92(2), 82-89. <http://dx.doi.org/10.1680/icien.1992.18771>.
- Chiu, C.F., Yan, W.M., & Yuen, K.V. (2012). Estimation of water retention curve of granular soils from particle-size distribution - A Bayesian probabilistic approach. *Canadian Geotechnical Journal*, 49(9), 1024-1035. <http://dx.doi.org/10.1139/t2012-062>.
- Delage, P., Audiguier, M., Cui, Y.J., & Deveughèle, M. (1995). Propriétés de rétention d'eau et Microstructure de différents géomatériaux. In Hanrahan (Ed.), *Proc. 9th European Conference on Soil Mechanics and Foundation Engineering* (pp. 43-48). Dublin, Ireland. CRC Press (in French).
- Fredlund, D.G., & Rahardjo, H. (1993). *Soil mechanics for unsaturated soils*. John Wiley & Sons. <https://doi.org/10.1002/9780470172759>
- Gao, Y., & Sun, D. (2017). Soil-water retention behavior of compacted soil with different densities over a wide suction range and its prediction. *Computers and Geotechnics*, 91, 17-26. <http://dx.doi.org/10.1016/j.compgeo.2017.06.016>.
- Gerscovich, D.M.S. (2001). Equations for modeling the soil-water characteristic curve applied to Brazilian soils. In W.Y.Y. Gehling, & F. Schnaid (Eds.), *Proc. 4th Brazilian Symposium on Unsaturated Soils*. (pp. 76-92), Porto Alegre. Palloti (in Portuguese).
- Gitirana, G.F.N., & Fredlund, D.G. (2004). Soil-water characteristic curve equation with independent properties. *Journal of Geotechnical and Geoenvironmental Engineering*, 130(2), 209-212. [http://dx.doi.org/10.1061/\(asce\)1090-0241\(2004\)130:2\(209\)](http://dx.doi.org/10.1061/(asce)1090-0241(2004)130:2(209)).
- Gonçalves F., Souza C.H.U., Tahira F.S., Fernandes F., & Teixeira R.S. (2017). Increment of sludge from water treatment plant in waterproofing barriers of sanitary landfill. *Revista DAE*, 65, 5-14 (in Portuguese). <https://doi.org/10.4322/dae.2016.018>

- Gonçalves, F., Correa, C.Z., Lopes, D.D., Vendrame, P.R.S., & Teixeira, R.S. (2019). Monitoring of the process of waste landfill leachate diffusion in clay and sandy soil. *Environmental Monitoring and Assessment*, 191, 577. <http://dx.doi.org/10.1007/s10661-019-7720-9>.
- Gonçalves, F., Zanin, R.F.B., Somera, L.F., Oliveira, A.D., Ferreira, J.W.S., Costa Branco, C.J.M., & Teixeira, R.S. (2018). Physical-chemical and mineralogical characterization of three soils in the state of Paraná. In *Proc. 19th Brazilian Congress of Soil Mechanics and Geotechnical Engineering*, Salvador, BA, Brazil. ABMS.
- Gutierrez, N.H.M., Nobrega, M.T., & Vilar, O.M. (2008). Influence of the microstructure in the collapse of a residual clayey tropical soil. *Bulletin of Engineering Geology and the Environment*, 68(1), 107-116. <http://dx.doi.org/10.1007/s10064-008-0180-z>.
- Kim, C.K., & Kim, T.H. (2010). Behavior of unsaturated weathered residual granite soil with initial water contents. *Engineering Geology*, 113(4), 1-10. <http://dx.doi.org/10.1016/j.enggeo.2009.09.004>.
- Li, X., & Zhang, L.M. (2009). Characterization of dual-structure pore-size distribution of soil. *Can Geotech*, 46(2), 129-141. <http://dx.doi.org/10.1139/t08-110>.
- Marinho, F.A.M. (1997). Soil suction measurement. In T.M.P. Campos, & E.A. Vargas Junior (Eds.), *Proc. 3rd Brazilian Symposium on Unsaturated Soils*. (pp. 373-397). Rio de Janeiro, RJ, Brazil. Freitas Bastos Editora (in Portuguese).
- Marinho, F.A.M. (2005). Nature of soil-water characteristic curve for plastic soils. *Journal of Geotechnical and Geoenvironmental Engineering*, 131(5), 654-661. [http://dx.doi.org/10.1061/\(ASCE\)1090-0241\(2005\)131:5\(654\)](http://dx.doi.org/10.1061/(ASCE)1090-0241(2005)131:5(654)).
- Marinho, F.A.M., Take, W.A., & Tarantino, A. (2008). Measurement of matric suction using tensiometric and axis translation techniques. *Geotechnical and Geological Engineering*, 26, 615. <http://dx.doi.org/10.1007/s10706-008-9201-8>.
- Mascarenha, M.M.A., Cordão-Neto, M.P., & Romero, E. (2010). Influence of the microstructure on the hydro-mechanical behaviour of a natural silty clay. In E. Alonso, & A. Gens (Eds.), *Unsaturated soils*, London, UK. CRC Press. <https://doi.org/10.1201/9781003026365>
- Miguel, M.G., & Bonder, B.H. (2012). Soil-water characteristic curves obtained for a colluvial and lateritic soil profile considering the macro and micro porosity. *Geotechnical and Geological Engineering*, 30(6), 1405-1420. <http://dx.doi.org/10.1007/s10706-012-9545-y>.
- Miguel, M.G., & Vilar, O.M. (2009). Study of the water retention properties of a tropical soil. *Canadian Geotechnical Journal*, 46(9), 1084-1092. <http://dx.doi.org/10.1139/t09-039>.
- Nimmo, J.R. (2005). Porosity and pore size distribution. In D. Hillel (Ed.), *Encyclopedia of Soils in the Environment*, (pp. 295-303). Academic Press. <https://doi.org/10.1016/B0-12-348530-4/00404-5>
- Nogami, J.S., & Villibor, D.F. (1981). A new soil classification for road purposes. In *Brazilian Symposium on Tropical Soils in Engineering*, (pp. 289-294). Rio de Janeiro, Brazil. COPPE/UFRJ, CNPq, ABMS (in Portuguese).
- Otalvaro, I.F., Cordão Neto, M.P., Delage, P., & Caicedo, B. (2016). Relationship between soil structure and water retention properties in a residual compacted soil. *Engineering Geology*, 205, 73-80. <http://dx.doi.org/10.1016/j.enggeo.2016.02.016>.
- Philip, J.R., & De Vries, D.A. (1957). Moisture movement in porous materials under temperature gradient. *Transactions: American Geophysical Union*, 38(2), 222-232. <http://dx.doi.org/10.1029/TR038i002p00222>.
- Rocha G.C., Barros O.N.F., & Guimarães M.F. (1991). Spatial distribution and soil characteristics of the campus of the State University of Londrina, PR. *Semina: Ciências Agrárias*, 12(1), 21-25 (in Portuguese). <https://doi.org/10.5433/1679-0359.1991v12n1p25>
- Romero, E., Gens, A., & Lloret, A. (1999). Water permeability, water retention and microstructure of unsaturated compacted Boom clay. *Engineering Geology*, 54(1-2), 117-127. [http://dx.doi.org/10.1016/S0013-7952\(99\)00067-8](http://dx.doi.org/10.1016/S0013-7952(99)00067-8).
- Romero, E., Gens, A., & Lloret, A. (2001). Temperature effects on the hydraulic behavior of an unsaturated clay. *Geotechnical and Geological Engineering*, 19(3), 311-332. <http://dx.doi.org/10.1023/A:1013133809333>.
- Sasanian, S., & Newson, T.A. (2013). Use of mercury intrusion porosimetry for microstructural investigation of reconstituted clays at high water contents. *Engineering Geology*, 158, 15-22. <http://dx.doi.org/10.1016/j.enggeo.2013.03.002>.
- Silva F.C., Cabral, S.M., Cabral, R.M., Carvalho, J.C., Cordão Neto, M.P., Oliveira, R.B., & Côrtes, H.A. (2020). Determination of the characteristic curve and influence of macro and micropores on a residual soil profile. *Geotecnia*, 149, 101-128 (in Portuguese). <http://doi.org/10.24849/j.geot.2020.149.06>
- Simms, P.H., & Yanful, E.K. (2001). Measurement and estimation of pore shrinkage and pore distribution in a clayey till during soil-water characteristic curve tests. *Canadian Geotechnical Journal*, 38(4), 741-754. <http://dx.doi.org/10.1139/t01-014>.
- Sun, D., You, G., Annan, Z., & Daichao, S. (2016). Soil-water retention curves and microstructures of undisturbed and compacted Guilin lateritic clay. *Bulletin of Engineering Geology and the Environment*, 75(2), 781-791. <http://dx.doi.org/10.1007/s10064-015-0765-2>.
- Tavakoli Dastjerdi, M.H., Habibagahi, G., & Nikooee, E. (2014). Effect of confining stress on soil water retention curve and its impact on the shear strength of unsaturated soils. *Vadose Zone Journal*, 13(5), 1-11. <http://dx.doi.org/10.2136/vzj2013.05.0094>.
- Teixeira, R.S., Cambier, P., Dias, R.D., Pinese, J.P.P., & Jaulin-Soubelet, A. (2010). Mobility of potentially harmful metals in latosols impacted by the municipal solid waste

- deposit of Londrina, Brazil. *Applied Geochemistry*, 25(1), 1-15. <http://dx.doi.org/10.1016/j.apgeochem.2009.09.022>.
- Vanapalli, S.K., Fredlund, D.G., Pufahl, D.E., & Clifton, A.W. (1996). Model for the prediction of shear strength with respect to soil suction. *Canadian Geotechnical Journal*, 33(3), 379-392. <http://dx.doi.org/10.1139/t96-060>.
- Vanapalli, S.K., Pufahl, D.E., & Fredlund, D.G. (1999). The effect of soil structure and stress history on the soil-water characteristics of a compacted till. *Geotechnique*, 49(2), 143-159. <http://dx.doi.org/10.1680/geot.1999.49.2.143>.
- Washburn, E.W. (1921). Note on a method of determining the distribution of pore sizes in a porous material. *Proceedings of the National Academy of Sciences of the United States of America*, 7(4), 115-116. <http://dx.doi.org/10.1073/pnas.7.4.115>.
- Yan, W., Birlle, E., & Cudmani, R. (2021). A simple approach for predicting soil water characteristic curve of clayey soils using pore size distribution data. *MATEC Web of Conferences*, 337: 02012. <https://doi.org/10.1051/mateconf/202133702012>
- Zhang, L., & Li, X. (2010). Microporosity structure of coarse granular soils. *Journal of Geotechnical and Geoenvironmental Engineering*, 136(10), 1425-1436. [http://dx.doi.org/10.1061/\(ASCE\)GT.1943-5606.0000348](http://dx.doi.org/10.1061/(ASCE)GT.1943-5606.0000348).
- Zhou, W.H., Yuen, K.V., & Tan, F. (2014). Estimation of soil-water characteristic curve and relative permeability for granular soils with different initial dry densities. *Engineering Geology*, 179, 1-9. <http://dx.doi.org/10.1016/j.enggeo.2014.06.013>.